Journal of Materials Chemistry C

RSC Publishing

PAPER

View Article Online
View Journal | View Issue

Cite this: J. Mater. Chem. C, 2013, 1, 4647

Highly efficient exciplex emission in solid-state light-emitting electrochemical cells based on mixed ionic hole-transport triarylamine and ionic electron-transport 1,3,5-triazine derivatives

Hsiao-Fan Chen,[a] Chih-Teng Liao,[b] Hai-Ching Su,*[b] Yun-Shiuan Yeh[a] and Ken-Tsung Wong*[a]

Received 20th March 2013
Accepted 24th May 2013

DOI: 10.1039/c3tc30518j

www.rsc.org/MaterialsC

Highly efficient exciplex emission in solid-state light-emitting electrochemical cells (LECs) was achieved by mixing two ionic fluorescent emitters with opposite bipolarity. A triarylamine derivative as a hole-transport material (HTM) and a 1,3,5-triazine derivative as an electron-transport material (ETM) were selected due to their superior carrier mobilities. The ionic character of HTM and ETM was achieved by chemically attaching three pendant methylimidazolium groups as peripheries, rendering them amenable to LEC applications. Strong exciplex green emission can be observed either from photoluminescence in solid states or electroluminescence in LEC devices when HTM and ETM are mixed. By optimizing the mixing ratio, the external quantum efficiency and power efficiency can be achieved up to 3.04% and 10.29 lm W^{-1}, respectively. These results are among the highest reported for fluorescent LECs.

Introduction

Organic light-emitting devices (OLEDs) have attracted much attention due to their promising potential in display and solid-state lighting applications.[1,2] To optimize the carrier injection and transport characteristics, hole-transport materials (HTM) and electron-transport materials (ETM) are often utilized simultaneously in either a single-layered blend device or a discrete multilayered device. When an HTM and an ETM are in close contact, either in a blend or at the interface between the thin films of the two materials, an exciplex can be formed through charge transfer in the excited states between the lowest unoccupied molecular orbital (LUMO) level of the acceptor and the highest occupied molecular orbital (HOMO) level of the donor.[3] Since exciplex emission is different from either the donor or the acceptor monomer emission, it offers a feasible way to tune the emission wavelength of OLEDs. Several single-color[4–11] and white[12–17] OLEDs based on exciplex emission have been reported. Although exciplex emission is generally weak and inefficient, several studies about efficient OLEDs based on exciplex emission were reported.[7,9–11,14,16–19] Good mobility balance and large offsets in energy levels of HTM and ETM have been pointed out to be important requirements for optimizing device efficiencies of exciplex-based OLEDs.[10] Similar carrier mobilities would increase the number of electron–hole pairs formed for exciplex emission at similar current densities. Large offsets in energy levels between HTM and ETM facilitate carrier accumulation at the HTM–ETM interface, enhancing the possibility for exciplex formation. With a judiciously chosen HTM–ETM pair, high external quantum efficiencies (EQE) >3% photons/electrons have been reported for exciplex-based OLEDs.[10]

In this work, we demonstrate efficient exciplex emission in light-emitting electrochemical cells (LECs). Compared with conventional OLEDs, solid-state LECs[20,21] possess several promising advantages. LECs generally require only a single emissive layer, which can be easily processed from solutions, and can conveniently use air-stable electrodes. The emissive layers of LECs contain mobile ions, which can drift toward electrodes under an applied bias. The spatially separated ions induce electrochemical doping (oxidation and reduction) of the emissive materials near the electrodes, *i.e.* p-type doping near the anode and n-type doping near the cathode.[20] The doped regions induce ohmic contacts with the electrodes and consequently facilitate the injection of both holes and electrons, which recombine at the junction between p- and n-type regions. As a result, a single-layered LEC device can be operated at very low voltages (close to E_g/e, where E_g is the energy gap of the emissive material and e is the elementary charge) with balanced carrier injection, giving high power efficiencies. Exciplex-based LECs employing a blend of p- and n-type luminescent conjugated polymers have been reported.[22] However, the EQE achieved in these devices is rather low (0.02%). To enhance the device efficiency of exciplex-based LECs, two novel ionic HTM

[a]Department of Chemistry, National Taiwan University, Taipei 10617, Taiwan. E-mail: kenwong@ntu.edu.tw; Fax: +886-2-33661667; Tel: +886-2-33661665

[b]Institute of Lighting and Energy Photonics, National Chiao Tung University, Tainan 71150, Taiwan. E-mail: haichingsu@mail.nctu.edu.tw; Fax: +886-6-3032535; Tel: +886-6-3032121-57792

and ETM are proposed to provide large offsets in energy levels for efficient exciplex formation. The design of HTM and ETM which are amenable for LEC application mainly requires introduction of movable ions. We simply attached three 1-methylimidazolium hexafluorophosphates in the terminal of alkyl peripheries onto the hole-transport tris(4-biphenyl)amine and electron-transport 2,4,6-tris(3-biphenyl)triazine to afford HTM and ETM, respectively. Both tris(4-biphenyl)amine and 2,4,6-tris(3-biphenyl)triazine have been proven to possess decent hole and electron mobilities of *ca.* 1.5×10^{-4} and 1.2×10^{-4} cm^2 V^{-1} s^{-1}, respectively.[23,24] In the mixed HTM–ETM emissive layer, balance of carrier mobility could be conveniently tailored by tuning the mixing ratio of the two materials. Hence, with balanced carrier transport and large offsets in energy levels at the HTM–ETM interface, high EQEs and power efficiencies up to 3% and 10 lm W^{-1}, respectively, can be obtained in single-layered fluorescent LECs based on exciplex emission.

Results and discussion

Synthesis

Scheme 1 outlines the syntheses of HTM and ETM. HTM-Br and ETM-Br were synthesized *via* modified one-pot Suzuki coupling of tris(4-bromophenyl)amine[25] and 2,4,6-tris(3-bromophenyl)triazine[24] with 1-bromo-4-(6-bromohexyl)benzene[26] in 39 and 41% yields, respectively. After treating HTM-Br and ETM-Br with an excess amount of 1-methylimidazole followed by ion-exchange with potassium hexafluorophosphate, we isolated HTM and ETM in 65 and 84% yields, respectively.

Electrochemical properties

Fig. 1 displays the electrochemical characteristics of HTM and ETM, as probed using cyclic voltammetry in acetonitrile. A reversible oxidation [at +0.43 V *vs.* (Fc/Fc^+)] was observed for HTM while ETM exhibited a reversible reduction [at −2.00 V *vs.* (Fc/Fc^+)]. Both oxidation and reduction occur at the core of the molecules. The supreme oxidation or reduction reversibility is attributed to the stable core structures of HTM (triarylamine) and ETM (1,3,5-triazine), making them good candidates for the formation of a stable charge-transfer complex in the excited state (exciplex). By adopting the reversible redox potentials, the HOMO of HTM and the LUMO of ETM can be calculated as −5.23 and −2.80 eV, respectively.

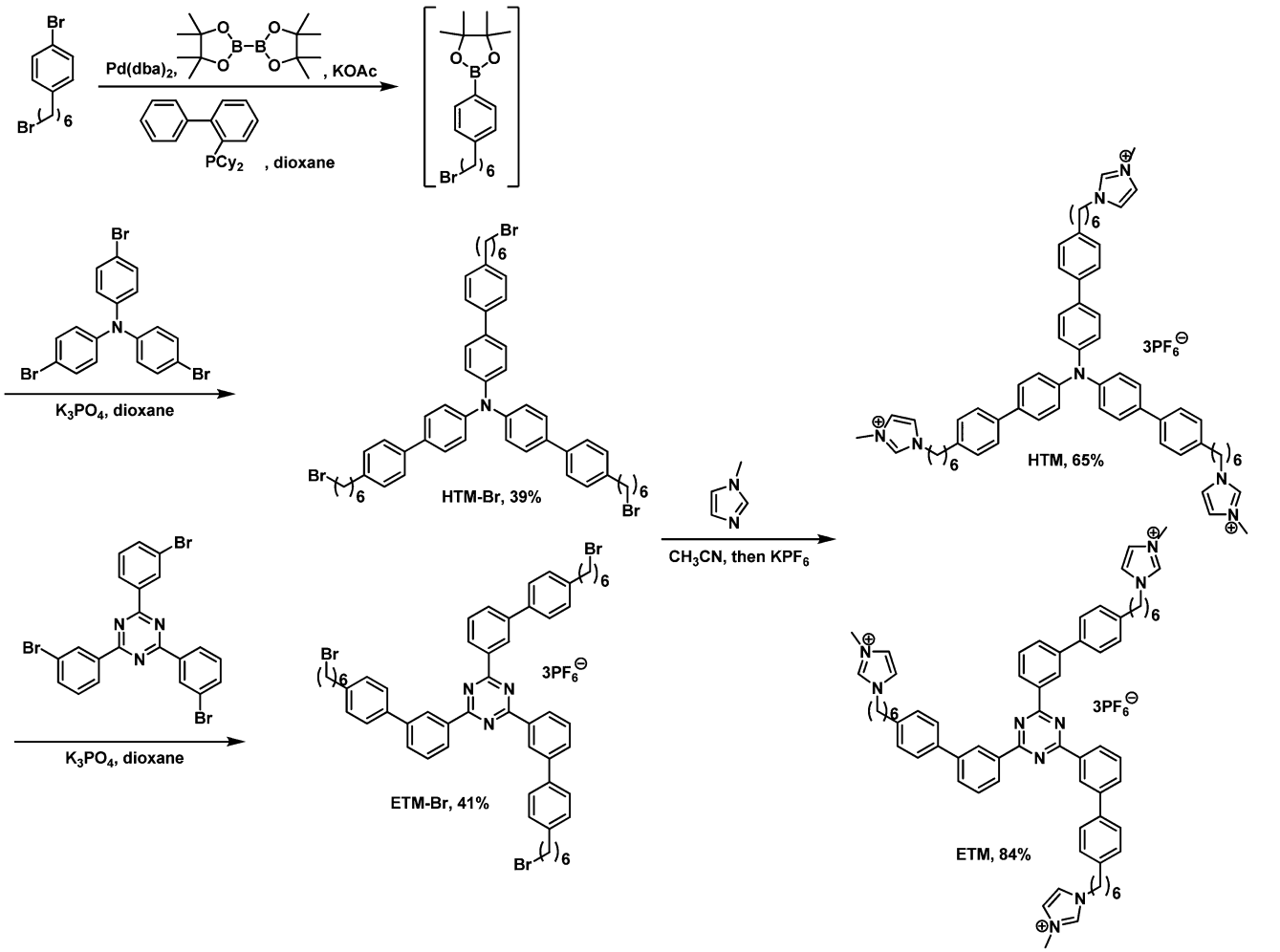

Scheme 1 Syntheses of HTM and ETM.

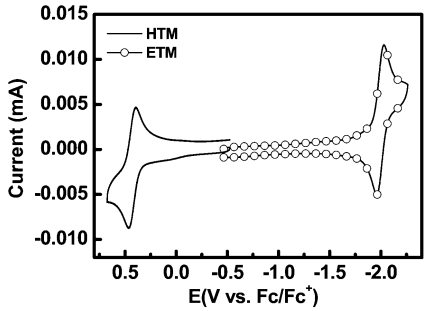

Fig. 1 Cyclic voltammograms of HTM and ETM. All potentials were recorded *vs.* Ag/AgCl (saturated) as a reference electrode and calibrated with the ferrocene/ferrocenium redox couple. A glassy carbon electrode was used as the working electrode; scan rate 100 mV s^{-1}.

Photoluminescence studies

Fig. 2a presents the UV-visible absorption and photoluminescence (PL) spectra of HTM and ETM in acetonitrile solutions (10^{-5} M). HTM shows two electronic transition bands at 270 and 340 nm. The shorter wavelength is assigned to be the electronic transition of biphenyl moieties and is red-shifted by ~25 nm as compared to that of tris(biphenyl-4-yl)-amine due to the introduction of alkyl peripheries, while the longer wavelength component is the electronic transition involving the entire amine moiety.[23] On the other hand, there is only one electronic transition band with λ_{max} at 264 nm for ETL which is consistent with the absorption regime of 2,4,6-triphenyltriazine derivatives.[24] The lack of the electronic transition at longer wavelengths indicates a limited conjugation between biphenyl and 1,3,5-triazine due to *meta*-conjugation. For solution PL, HTM and ETM exhibited similar structureless fluorescence at 423 and 428 nm with PL quantum yields of 0.49 and 0.06, respectively. Both absorption and PL spectra of HTM : ETM with 1 : 1 weight ratio are approximately the superposition of individual spectra, showing no indication of intermolecular interaction between HTM and ETM presumably due to insufficient concentration. In films (Fig. 2b), the absorption spectrum of HTM exhibited comparable peak intensities at 265 and 350 nm as compared to those in the acetonitrile solution. The change in relative peak intensities might be due to the overall effect of different degrees of molecular flexibility in solutions and in films and as well as the dielectric environment, causing different oscillator strengths in their electronic transitions.[27,28] Notably, ETM showed a red-shifted absorption peak at 280 nm with a significantly broadened tail from 370 nm to 600 nm, indicating a great extent of intermolecular interaction due to a better planarity of the 2,4,6-triphenyltriazine core structure. The absorption spectrum of the mixed sample with 1 : 1 weight ratio in thin film showed no sign of intermolecular interaction between HTM and ETM in the ground state.

PL spectra of thin films containing various mixing weight ratios of HTM–ETM on quartz substrates are shown in Fig. 2c. The PL emission peaks of pure ETM and HTM films are 400 and 425 nm, respectively. It is noted that some excimer emission around 550 nm was observed in the PL spectrum of pure ETM films. The appearance of excimer emission from ETM films is

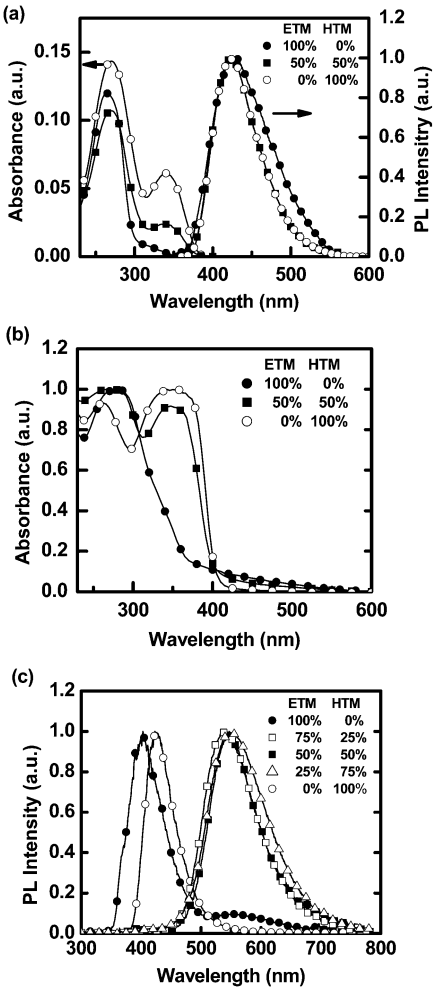

Fig. 2 Absorption and/or PL spectra of HTM and ETM with various mixing weight ratios in acetonitrile solution (10^{-5} M) (a) and thin films on quartz substrates [(b) and (c)].

evidence for the substantial intermolecular interaction, in line with the observation of the significantly broadened tail after 370 nm in the solid-state absorption spectrum. When the two materials are mixed, the PL emission of the pristine films is totally quenched and a new emission band centered at 545 nm is observed. To clarify this phenomenon, the HOMO and LUMO levels of both materials estimated by CV measurements as well as the energy gaps estimated from the absorption onset of the solid films are depicted in Fig. 3. Deep-blue emission of the pristine films is attributed to deactivation of the monomer excited states of ETM and HTM. The new green emission would be inferred to the emission of exciplex formed between ETM and HTM. The energy gap of exciplex emission is determined by the energy difference between the LUMO level of the acceptor molecule and the HOMO level of the donor molecule. As shown in Fig. 3, the photon energy of exciplex emission can be estimated to be 2.43 eV, which matches well with the measured value (2.28 eV, Fig. 1). Slightly smaller energy gaps in thin films as compared to those in solutions are due to the environmental polarization. To further examine the new emission band, the intermolecular distance between HTM and ETM was adjusted

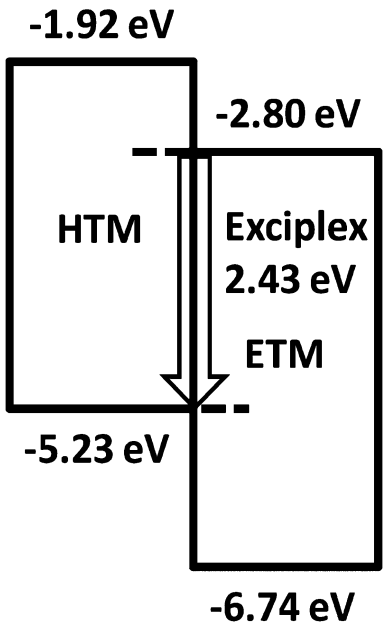

Fig. 3 Energy levels of HTM and ETM.

by dispersing the HTM–ETM mixture (HTM : ETM = 1 : 3, weight ratio) in poly(methylmethacrylate) (PMMA) films. As shown in Fig. 4, the relative amount of new green emission with respect to the monomer emission reduces as the PMMA concentration increases. It reveals that steric hindrance provided by an inert polymer matrix effectively suppresses the new green emission. Such results further confirm that the green emission arises from HTM–ETM exciplex emission.

Electroluminescence studies

To study the electroluminescence (EL) properties of exciplex-based LECs, EL characteristics of LEC devices based on emissive layers containing various mixing ratios of HTM and ETM were measured and are summarized in Table 1. The LECs have the structure of indium tin oxide (ITO) (120 nm)/poly(3,4-ethylenedioxythiophene):poly(styrene sulfonate) (PEDOT:PSS) (30 nm)/emissive layer (200 nm)/Ag (100 nm). Emissive layers containing ETM concentrations of 100, 75, 50, 25 and 0 wt% are denoted as Devices **E100**, **E75**, **E50**, **E25** and **E0**, respectively. The EL spectra of LEC devices based on emissive layers containing various mixing weight ratios of HTM and ETM are depicted in Fig. 5. The EL spectrum of the pure HTM device (**E0**) resembles the PL spectrum of pure HTM films (Fig. 2c). However, ETM shows significantly different PL and EL spectra. The monomer emission band in the blue region is suppressed and the excimer emission band in the green region is significantly enhanced (*cf.* Fig. 2c and 5). This phenomenon may be related to self-heating of the EL devices during operation.[29] It would result in a spatial rearrangement of molecules and consequently promote the formation of intermolecular excimer species. When HTM and ETM are mixed, the EL spectra are insensitive to the mixing ratios and are in good agreement with the PL spectra of mixing films (*cf.* Fig. 2c and 5). It is noted that

Table 1 Summary of the LEC device characteristics

Device (ETM concentration)	Bias (V)	t_{max}[a] (min)	L_{max}[b] (cd m^{-2})	$\eta_{ext,max}$[c] (%)	$\eta_{p,max}$[d] (lm W^{-1})	Lifetime[e] (min)
E100 (100 wt%)	3.8 V	13.8	0.01	0.13	0.33	9.3
	4.2 V	12.7	0.02	0.15	0.35	5.7
	4.6 V	8.8	0.03	0.20	0.42	3.6
E75 (75 wt%)	3.0 V	12.1	0.29	3.04	10.29	10.0
	3.4 V	5.9	0.54	2.98	8.89	19.6
	3.8 V	5.8	0.75	2.56	6.85	17.1
	4.2 V	4.6	1.17	2.61	6.30	9.6
	4.6 V	3.5	1.61	2.67	5.89	6.8
E50 (50 wt%)	3.8 V	3.5	9.69	0.90	2.45	1.2
	4.2 V	3.5	10.15	0.79	1.97	1.1
	4.6 V	2.0	12.87	0.78	1.76	0.8
E25 (25 wt%)	3.8 V	2.3	2.35	0.08	0.20	12.0
	4.2 V	1.4	3.31	0.09	0.21	10.4
	4.6 V	1.2	4.13	0.08	0.18	9.3
E0 (0 wt%)	3.8 V	18.3	0.09	0.0074	0.0034	21.2
	4.2 V	14.1	0.21	0.0047	0.0020	14.9
	4.6 V	11.3	0.27	0.0058	0.0022	11.4

[a] Time required to reach the maximal brightness. [b] Maximal brightness achieved at a constant bias voltage. [c] Maximal external quantum efficiency achieved at a constant bias voltage. [d] Maximal power efficiency achieved at a constant bias voltage. [e] The time for the brightness of the device to decay from the maximum to half of the maximum under a constant bias voltage.

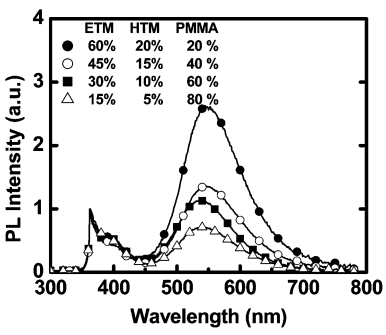

Fig. 4 PL spectra of thin films of a HTM–ETM mixture (HTM : ETM = 1 : 3, weight ratio) dispersed in PMMA on quartz substrates.

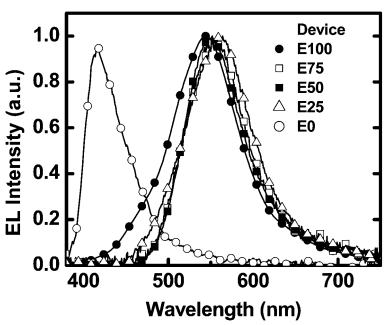

Fig. 5 EL spectra of LEC devices based on emissive layers containing various mixing weight ratios of HTM and ETM. Devices with ETM concentrations of 100, 75, 50, 25 and 0 wt% are denoted as **E100**, **E75**, **E50**, **E25** and **E0**, respectively.

the EL spectrum of devices with a mixed HTM–ETM emissive layer is red-shifted as compared to that of pure ETM devices (Fig. 5). Hence, it reveals different mechanisms responsible for EL emissions of mixed HTM–ETM and pure ETM devices. The EL emission of mixed HTM–ETM devices arises from HTM–ETM exciplex emission while excimer emission dominates the EL spectrum of pure ETM devices.

All LECs based on various mixing ratios of HTM and ETM showed similar time-dependent EL characteristics. The time-dependent brightness and current density of Device **E75** under a constant bias of 3.0 V are shown in Fig. 6a. After the bias was applied, the device current monotonically rose and then gradually decreased with time. On the other hand, the brightness first increased with the device current, reaching a local maximum value before undergoing a gradual decrease to a local minimum value at *ca.* 7.5 min. Then the brightness rose again and reached the maximum value. Finally, the brightness monotonically decreased with the device current. The reason for the second rise in brightness will be explained later. The time required for the brightness to reach its maximum value decreased as the bias voltage increased (Table 1) due to a higher accumulation rate of mobile ions to facilitate the formation of electrochemically doped regions under a higher electric field. It is noted that the device response of mixed HTM–ETM devices (**E75**, **E50** and **E25**) was faster than that of pure HTM (**E0**) or ETM (**E100**) devices (Table 1). A mixed HTM–ETM emissive layer would facilitate carrier injection as compared to pure films of HTM and ETM (Fig. 3). Fewer accumulated ions near electrodes are consequently required to significantly enhance carrier injection, accelerating device turn-on.[30] After reaching the maximum brightness, the brightness then dropped with time with a rate depending on the bias voltage. Under a constant bias, the lifetime of each device, defined as the time required for the brightness of the device to decay from the maximum value to half of the maximum value, decreased upon increasing the bias voltage (Table 1). It results from the fact that a higher current density induced by a higher bias voltage leads to a higher rate of irreversible multiple oxidation and subsequent decomposition of the emissive material, thereby accelerating the degradation of the LEC devices.[31]

The EQE and power efficiency of Device **E75** under a constant bias of 3.0 V are shown in Fig. 6b. Immediately after a forward bias was applied, the EQE was rather low because of unbalanced carrier injection. During the formation of the doped regions near the electrodes, the balance of the carrier injection improved and, accordingly, the EQE of the device increased rapidly. The peak EQE and peak power efficiency for Device **E75** under 3.0 V were 3.04% and 10.29 lm W^{-1}, respectively. After reaching the peak device efficiency, the device current was still increasing while the brightness was decreasing. Thus, the device efficiency deteriorated rapidly. Before the doped regions were well established, *i.e.*, the device current was still increasing, the thickness of the intrinsic layer between the p- and n-type doped layers gradually reduced and thus the electric field in the intrinsic layer increased with time.[32] The recombination zone in the intrinsic layer may keep moving due to field-dependent carrier mobilities and gradually formed doped layers, which enhance carrier injection efficiency with time. The brightness and device efficiency would reduce as the recombination zone approaches electrodes due to exciton quenching near the doped regions[33–35] while the brightness and device efficiency would recover when the recombination zone moves away from electrodes. However, the recovered device efficiency would not be as high as the maximum value due to the degradation of the emissive material during the LEC operation.[36] Similar dual-peak characteristics in brightness and device efficiency were also observed in LECs with thicker emissive layers (>200 nm).[37,38] Compared with a thinner emissive layer, a thicker emissive layer is beneficial in keeping the recombination zone away from the doped regions. Since exciton quenching reduces when the recombination zone is moving toward the center of the emissive layer, recovering of brightness and device efficiency can be measured in such devices.

Maximum brightness as a function of maximum current density for all LEC devices is shown in Fig. 7. The device current under similar bias voltages (3.8–4.6 V) increases significantly as the percentage of the HTM concentration increases. It reveals that the hole mobility of HTM would be higher than the electron mobility of ETM. The brightness first increases as the proportion of HTM increases and then decreases when the percentage of HTM concentration exceeds 50%. Increase in brightness as the proportion of HTM increases results from improved carrier balance in the mixed ETM–HTM layer. However, further increase in HTM concentration deteriorates carrier balance and thus device efficiency significantly reduces (Table 1), rendering lowered brightness.

Although the EL spectra of the mixed HTM–ETM LECs were insensitive to the mixing ratios, the device efficiency is strongly

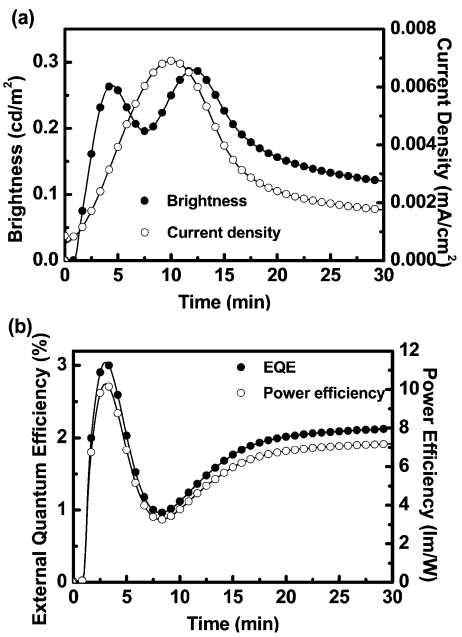

Fig. 6 (a) Brightness (solid symbols) and current density (open symbols) and (b) EQE (solid symbols) and power efficiency (open symbols) plotted with respect to time under a constant bias voltage of 3.0 V for Device **E75**.

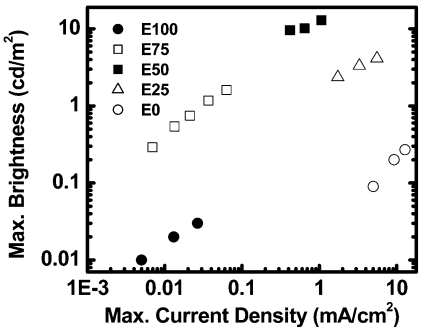

Fig. 7 Maximum brightness as a function of maximum current density for all LEC devices.

dependent on the mixing ratios (Table 1). For pure HTM and ETM devices, the device current would be predominantly unipolar and thus the recombination zone would be located near doped regions, resulting in severe exciton quenching and rather low device efficiencies. In devices based on emissive layers containing mixed hole- and electron-transport materials, carrier balance would be better and thus the recombination zone would be pushed away from doped regions. As a result, exciton quenching near the doped regions would be reduced and the device efficiency can be improved. When 25 wt% ETM was mixed in pure HTM LECs, an order of magnitude in enhancement of EQE can be obtained (*cf.* Devices **E25** and **E0**, Table 1). Further order-of-magnitude enhancement of EQE was measured by increasing the concentration of ETM to 50 wt% (*cf.* Devices **E50** and **E25**, Table 1). Finally, the EQE achieved in the device based on 75 wt% ETM was up to *ca.* 2.6%, which is over 350× increment in device efficiency as compared to that of pure HTM devices under similar bias voltages (3.8–4.6 V) (*cf.* Devices **E75** and **E0**, Table 1). With this optimized mixing ratio, even higher EQE and power efficiency up to *ca.* 3.0% and 10.3 lm W^{-1} were measured by lowering the bias voltage to 3.0 V. These results are among the highest reported for fluorescent LECs. Therefore, it confirms that efficient LECs based on exciplex emission can be realized by simultaneously adopting two strategies: (i) a suitable HTM–ETM pair should be judiciously chosen to provide a large energy level offset for efficient exciplex formation; (ii) to optimize device efficiency, balance of carrier mobility could then be tailored by tuning the mixing ratio of the two materials.

Recently, enhanced singlet exciplex emission from OLEDs has been reported.[39,40] It was achieved by production of singlets *via* triplet–triplet annihilation, *i.e.*, triplet fusion[39] or thermally assisted delayed fluorescence.[40] The latter takes place in emitters with a small singlet–triplet gap (small electron exchange energy), which facilitates triplets to undergo reverse intersystem crossing back into the singlet manifold. Efficient exciplex emission in LECs based on the HTM–ETM pair reported in this work may also result partially from the two mechanisms shown above. However, triplet fusion would more likely be responsible for enhanced singlet exciplex emission since the singlet–triplet gaps for ETM and HTM (0.16 and 0.38 eV, respectively) are not small enough to efficiently activate reverse intersystem crossing.

Conclusion

In summary, we have designed and synthesized ionic HTM and ETM by chemically attaching three pendant methylimidazolium groups as peripheries of hole-transport tris(4-biphenyl)amine and electron-transport 2,4,6-tris(3-biphenyl)triazine, respectively. The ionic character of HTM and ETM renders them amenable to LEC application. The core structures of HTM and ETM possess excellent electrochemical reversibility for oxidation and reduction, as well as high hole and electron mobilities, respectively, potential to generate efficient exciplex emission when HTM and ETM are mixed in the solid state. We observed a new green emission band centered at 545 nm in the mixed film with weight ratio of HTM and ETM ranging from 3 : 1 to 1 : 3. The green emission can also be suppressed by the addition of the inert polymer matrix PMMA, indicating that the green emission arises from HTM–ETM exciplex. The EL properties of exciplex-based LECs have been examined by incorporating the HTL emissive layers containing ETM concentrations of 100, 75, 50, 25 and 0 wt%. The EL spectra of the mixed HTM–ETM LECs are insensitive to the mixing ratios and are in good agreement with the PL spectra of mixed films. However, the device efficiency is strongly dependent on the mixing ratios. In devices based on emissive layers containing mixed hole- and electron-transport materials, carrier balance would be better and thus the recombination zone would be pushed away from doped regions. By optimizing the mixing ratio, the EQE and power efficiency can be achieved up to 3.04% and 10.29 lm W^{-1}, respectively. These results are among the highest reported for fluorescent LECs. Therefore, we believe that efficient LECs based on exciplex emission can be obtained by two simple strategies – judicious selection of the HTM–ETM pair to provide large energy level offset and tuning the mixing ratio of the two materials to balance the carrier mobility.

Experimental section

General experiments

^{1}H and ^{13}C NMR spectra of compounds were collected on a 400 MHz spectrometer at room temperature. Redox potentials of all complexes were determined by cyclic voltammetry (CV) at a scan rate of 100 mV s^{-1} in acetonitrile solution (1.0 mM). A glassy carbon electrode and a platinum wire were used as the working electrode and the counter electrode, respectively. All potentials were recorded *versus* the Ag/AgCl (saturated) reference electrode and calibrated with the ferrocene/ferrocenium redox couple. Oxidation CV was performed using 0.1 M tetra-*n*-butylammonium hexafluorophosphate ($TBAPF_6$) in acetonitrile as the supporting electrolyte. For reduction CV, 0.1 M tetra-*n*-butylammonium perchlorate (TBAP) in acetonitrile was used as the supporting electrolyte. Photophysical characteristics of HTM and ETM in solutions were measured at room temperature by using acetonitrile solutions (10^{-5} M) of all compounds. The thickness of spin-coated films measured by profilometry is 200 nm. UV-visible absorption spectra were recorded on a spectrophotometer (HITACHI U2800A). PL spectra were measured with a fluorescence spectrophotometer (HITACHI F9500).

Synthesis of tris(4′-(6-bromohexyl)biphenyl-4-yl)amine (HTM-Br). A mixture of 1-bromo-4-(6-bromohexyl)benzene (1.94 g, 6.06 mmol), bis(pinacolato)diborane (1.54 g, 6.06 mmol, donated by Frontier Scientific), bis(dibenzylideneacetone)-palladium(0) (27 mg, 0.03 mmol), biphenyl-2-yl-dicyclohexyl-phosphane (42 mg, 0.12 mmol), potassium acetate (1.19 g, 12.1 mmol), and dioxane (20 mL) was refluxed for 15 min. A suspension of tris(4-bromophenyl)amine (964 mg, 2.00 mmol) and potassium phosphate (7.72 g, 36.3 mmol) in dioxane (10 mL) and deionized water (15 mL) was added to the solution and refluxed for a further 1.5 h. After dioxane was removed by rotary evaporation, the reaction mixture was extracted with CH_2Cl_2 and dried over $MgSO_4$. The crude product was purified by column chromatography on silica gel (CH_2Cl_2/hexane = 1/4) to afford a pure product (748 mg, 39%) as a sticky colorless liquid. ^{1}H NMR (CD_2Cl_2, 400 MHz) δ 7.55–7.52 (m, 12H), 7.26 (d, J = 8.0 Hz, 6H), 7.22 (d, J = 8.0 Hz, 6H), 3.45 (t, J = 6.8 Hz, 6H), 2.67 (t, J = 8.0 Hz, 6H), 1.89 (quin., J = 6.8 Hz, 6H), 1.68 (quin., J = 7.2 Hz, 6H), 1.54–1.39 (m, 12H); ^{13}C NMR (CD_2Cl_2, 100 MHz) δ 146.6, 141.3, 137.9, 135.4, 128.7, 127.6, 126.5, 124.3, 35.3, 33.9, 32.7, 31.1, 28.3, 28.0; HRMS (m/z, FAB$^+$) calcd for $C_{54}H_{60}{}^{79}Br_3N$ 959.2276, found: 959.2285; calcd for $C_{54}H_{60}{}^{79}Br_2{}^{81}BrN$ 961.2255, found: 961.2277; calcd for $C_{54}H_{60}{}^{79}Br^{81}Br_2N$ 963.2235, found: 963.2212; calcd for $C_{54}H_{60}{}^{81}Br_3N$ 965.2214, found: 965.2202.

Synthesis of tris(4′-(6-(3-methylimidazolium)hexyl)biphenyl-4-yl)amine tris(hexafluorophosphate) (HTM). A mixture of tris(4′-(6-bromohexyl)biphenyl)-4-ylamine (636 mg, 0.66 mmol) and 1-methylimidazole (0.17 mL, 2.18 mmol) was dissolved in acetonitrile (3 mL) and refluxed for 12 h. The reaction mixture was concentrated and extracted with CH_2Cl_2 and aqueous solution of potassium hexafluorophosphate (30 mL, 0.13 M). The crude product was purified by column chromatography on alumina (ACN/CH_2Cl_2 = 1/9 to 9/1) to afford a pure product (600 mg, 65%) as a white solid. ^{1}H NMR (DMSO-d_6, 400 MHz) δ 9.06 (s, 3H), 7.73 (s, 3H), 7.66 (s, 3H), 7.60 (d, J = 8.0 Hz, 6H), 7.54 (d, J = 8.0 Hz, 6H), 7.24 (d, J = 8.0 Hz, 6H), 7.12 (d, J = 8.0 Hz, 6H), 4.13 (t, J = 6.8 Hz, 6H), 3.83 (s, 9H), 2.59 (t, J = 6.8 Hz, 6H), 1.80 (quin., J = 6.8 Hz, 6H), 1.59 (quin., J = 6.8 Hz, 6H), 1.31–1.28 (m, 12H); ^{13}C NMR (DMSO-d_6, 100 MHz) δ 146.1, 141.1, 137.0, 136.5, 134.7, 128.9, 127.5, 126.1, 124.1, 123.6, 122.3, 48.8, 35.7, 34.6, 30.6, 29.3, 28.0, 25.4; HRMS (m/z, ESI$^+$) calcd for $C_{66}H_{78}F_{18}N_7P_3$ 1403.5228, found: 1403.5210.

Synthesis of 2,4,6-tris(4′-(6-bromohexyl)biphenyl-3-yl)-triazine (ETM-Br). A mixture of 1-bromo-4-(6-bromohexyl)-benzene (1.78 g, 5.55 mmol), bis(pinacolato)diborane (1.41 g, 5.55 mmol, donated by Frontier Scientific), bis(dibenzylide-neacetone)palladium(0) (25 mg, 0.03 mmol), biphenyl-2-yl-dicyclohexylphosphane (39 mg, 0.11 mmol), potassium acetate (1.09 g, 11.1 mmol), and dioxane (20 mL) was refluxed for 30 min. A suspension of 2,4,6-tris(3-bromophenyl)triazine (1 g, 1.83 mmol) and potassium phosphate (7.07 g, 33.3 mmol) in dioxane (10 mL) and deionized water (15 mL) was added to the solution and refluxed for further 1 h. After dioxane was removed by rotary evaporation, the reaction mixture was extracted with CH_2Cl_2 and dried over $MgSO_4$. The crude product was purified by column chromatography on silica gel ($CHCl_3$/hexane = 1/2) to afford a pure product (700 mg, 41%) as a sticky colorless liquid. ^{1}H NMR ($CDCl_3$, 400 MHz) δ 9.00 (s, 3H), 8.74 (d, J = 8.0 Hz, 3H), 7.84 (d, J = 8.0 Hz, 3H), 7.68–7.63 (m, 9H), 7.33 (d, J = 8.0 Hz, 6H), 3.43 (t, J = 6.8 Hz, 6H), 2.71 (t, J = 8.0 Hz, 6H), 1.90 (quin., J = 6.8 Hz, 6H), 1.73 (quin., J = 7.2 Hz, 6H), 1.58–1.41 (m, 12H); ^{13}C NMR ($CDCl_3$, 100 MHz) δ 171.8, 142.1, 141.6, 138.3, 136.8, 131.1, 129.1, 129.0, 127.7, 127.5, 127.2, 35.5, 33.9, 32.7, 31.3, 28.5, 28.0; HRMS (m/z, FAB$^+$) calcd for $C_{57}H_{60}{}^{79}Br_3N_3$ 1023.2337, found: 1023.2327; calcd for $C_{57}H_{60}{}^{79}Br_2{}^{81}BrN_3$ 1025.2317, found: 1025.2291; calcd for $C_{57}H_{60}{}^{79}Br^{81}Br_2N_3$ 1027.2296, found: 1027.2267; calcd for $C_{57}H_{60}{}^{81}Br_3N_3$ 1029.2276, found: 1029.2268.

Synthesis of 2,4,6-tris(4′-(6-(3-methylimidazolium)hexyl)-biphenyl-3-yl)triazine tris(hexafluorophosphate) (ETM). A mixture of 2,4,6-tris(4′-(6-bromohexyl)biphenyl-4-yl)triazine (650 mg, 0.62 mmol) and 1-methylimidazole (0.17 mL, 2.55 mmol) was dissolved in acetonitrile (3 mL) and refluxed for 12 h. The reaction mixture was concentrated and a solution of potassium hexafluorophosphate (700 mg, 3.80 mmol) in deionized water (30 mL) was added and stirred for 10 min. The appeared solid was washed with deionized water and collected to afford a pure compound (780 mg, 84%) as a white solid. ^{1}H NMR (DMSO-d_6, 400 MHz) δ 9.07 (s, 3H), 8.93 (s, 3H), 8.73 (d, J = 8.0 Hz, 3H), 7.99 (d, J = 8.0 Hz, 3H), 7.76–7.72 (m, 12H), 7.68 (s, 3H), 7.37 (d, J = 8.0 Hz, 6H), 4.14 (t, J = 7.2 Hz, 6H), 3.83 (s, 9H), 2.65 (t, J = 8.0 Hz, 6H), 1.79 (quin., J = 7.2 Hz, 6H), 1.63 (quin., J = 7.2 Hz, 6H), 1.37–1.30 (m, 12H); ^{13}C NMR (DMSO-d_6, 100 MHz) δ 171.6, 142.5, 141.3, 137.5, 136.9, 136.5, 131.6, 130.2, 129.5, 128.0, 127.2, 126.9, 124.0, 122.7, 49.2, 36.1, 35.1, 31.0, 29.7, 28.4, 25.8; HRMS (m/z, ESI$^+$) calcd for $C_{69}H_{78}N_9{}^{3+}$ 1032.6380, found: 1032.6381.

Fabrication and characterization of LEC devices

ITO-coated glass substrates were cleaned and treated with UV/ozone prior to use. A poly(3,4-ethylenedioxythiophene): poly(styrene sulfonate) (PEDOT:PSS) layer (30 nm) was spin-coated onto the ITO substrate in air and then the structure was baked at 150 °C for 30 min. The emissive layers were then spin-coated from an acetonitrile solution containing various mixing weight ratios of HTM and ETM (HTM : ETM = 0 : 100, 25 : 75, 50 : 50, 75 : 25 and 100 : 0 for Devices **E100**, **E75**, **E50**, **E25** and **E0**, respectively) with a solute concentration of 150 mg mL^{-1}. The thickness of the emissive layer is *ca.* 200 nm. Preparation and spin-coating processes of all solutions were carried out under ambient conditions. After spin-coating the emissive layer, the samples were baked at 70 °C for 10 h in a nitrogen glove box (oxygen and moisture levels below 1 ppm) and then subjected to thermal evaporation under a 100 nm thick Ag top contact in a vacuum chamber (*ca.* 10^{-6} torr). The electrical and emission characteristics of the LEC devices were measured using a source-measurement unit and a Si photodiode calibrated with a Photo Research PR-650 spectroradiometer. All device measurements were performed under a constant bias voltage in a nitrogen glove box. EL spectra of LEC devices were recorded using a calibrated CCD spectrograph.

References

1 H. Burroughes, D. D. C. Bradley, A. R. Brown, R. N. Marks, K. Mackay, R. H. Friend, P. L. Burn and A. B. Holmes, *Nature*, 1990, **347**, 539.
2 C. W. Tang and S. A. Van Slyke, *Appl. Phys. Lett.*, 1987, **51**, 913.
3 S. A. Jenekhe and J. A. Osaheni, *Science*, 1994, **265**, 765.
4 J.-F. Wang, Y. Kawabe, S. E. Shaheen, M. M. Morrell, G. E. Jabbour, P. A. Lee, J. Anderson, N. R. Armstrong, B. Kippelen, E. A. Mash and N. Peyghambarian, *Adv. Mater.*, 1998, **10**, 230.
5 K. Itano, H. Ogawa and Y. Shirota, *Appl. Phys. Lett.*, 1998, **72**, 636.
6 K. Okumoto and Y. Shirota, *J. Lumin.*, 2000, **87**, 1171.
7 M. Cocchi, D. Virgili, G. Giro, V. Fattori, P. Di Marco, J. Kalinowski and Y. Shirota, *Appl. Phys. Lett.*, 2002, **80**, 2401.
8 X. Jiang, M. S. Liu and A. K.-Y. Jen, *J. Appl. Phys.*, 2002, **91**, 10147.
9 L. C. Palilis, A. J. Mäkinen, M. Uchida and Z. H. Kafafi, *Appl. Phys. Lett.*, 2003, **82**, 2209.
10 S. L. Lai, M. Y. Chan, Q. X. Tong, M. K. Fung, P. F. Wang, C. S. Lee and S. T. Lee, *Appl. Phys. Lett.*, 2008, **93**, 143301.
11 D. Wang, W. Li, B. Chu, Z. Su, D. Bi, D. Zhang, J. Zhu, F. Yan, Y. Chen and T. Tsuboi, *Appl. Phys. Lett.*, 2008, **92**, 053304.
12 C.-I. Chao and S.-A. Chen, *Appl. Phys. Lett.*, 1998, **73**, 426.
13 J. Feng, F. Li, W. Gao, S. Liu, Y. Liu and Y. Wang, *Appl. Phys. Lett.*, 2001, **78**, 3947.
14 S. Chen, Z. Wu, Y. Zhao, C. Li, J. Hou and S. Liu, *Org. Electron.*, 2005, **6**, 111.
15 D. Wang, W. L. Li, Z. S. Su, T. L. Li, B. Chu, D. F. Bi, L. L. Chen, W. M. Su and H. He, *Appl. Phys. Lett.*, 2006, **89**, 233511.
16 Y. M. Kim, Y. W. Park, J. H. Choi, B. K. Jub, J. H. Jung and J. K. Kim, *Appl. Phys. Lett.*, 2007, **90**, 033506.
17 S.-L. Lai, Q.-X. Tong, M.-Y. Chan, T.-W. Ng, M.-F. Lo, S.-T. Lee and C.-S. Lee, *J. Mater. Chem.*, 2011, **21**, 1206.
18 K. Goushi, K. Yoshida, K. Sato and C. Adachi, *Nat. Photonics*, 2012, **6**, 253.
19 K. Goushi and C. Adachi, *Appl. Phys. Lett.*, 2012, **101**, 023306.
20 Q. Pei, G. Yu, C. Zhang, Y. Yang and A. J. Heeger, *Science*, 1995, **269**, 1086.
21 R. D. Costa, E. Ortí, H. J. Bolink, F. Monti, G. Accorsi and N. Armaroli, *Angew. Chem., Int. Ed.*, 2012, **51**, 8178.
22 Y. Yang and Q. Pei, *Appl. Phys. Lett.*, 1997, **70**, 1926.
23 H. Inada, K. Ohnishi, S. Nomura, A. Higuchi, H. Nakano and Y. Shirota, *J. Mater. Chem.*, 1994, **4**, 171.
24 H.-F. Chen, S.-J. Yang, Z.-H. Tsai, W.-Y. Hung, T.-C. Wang and K.-T. Wong, *J. Mater. Chem.*, 2009, **19**, 8112.
25 D. Sahu, C.-H. Tsai, H.-Y. Wei, K.-C. Ho, F.-C. Chang and C.-W. Chu, *J. Mater. Chem.*, 2012, **22**, 7945.
26 E. Bacher, S. Jungermann, M. Rojahn, V. Wiederhirn and O. Nuyken, *Macromol. Rapid Commun.*, 2004, **25**, 1191.
27 L. M. Lawson-Daku, J. Linares and M.-L. Boillot, *Phys. Chem. Chem. Phys.*, 2010, **12**, 6107.
28 M. I. Sancho, M. C. Almandoz, S. E. Blanco and E. A. Castro, *Int. J. Mol. Sci.*, 2011, **12**, 8895.
29 Q. Sun, X. Zhan, C. Yang, Y. Liu, Y. Li and D. Zhu, *Thin Solid Films*, 2003, **440**, 247.
30 C.-T. Liao, H.-F. Chen, H.-C. Su and K.-T. Wong, *Phys. Chem. Chem. Phys.*, 2012, **14**, 9774.
31 S. T. Parker, J. D. Slinker, M. S. Lowry, M. P. Cox, S. Bernhard and G. G. Malliaras, *Chem. Mater.*, 2005, **17**, 3187.
32 M. Lenes, G. Garcia-Belmonte, D. Tordera, A. Pertegás, J. Bisquert and H. J. Bolink, *Adv. Funct. Mater.*, 2011, **21**, 1581.
33 D. J. Dick, A. J. Heeger, Y. Yang and Q. Pei, *Adv. Mater.*, 1996, **8**, 985.
34 C.-T. Liao, H.-F. Chen, H.-C. Su and K.-T. Wong, *Phys. Chem. Chem. Phys.*, 2012, **14**, 1262.
35 C.-T. Liao, H.-F. Chen, H.-C. Su and K.-T. Wong, *J. Mater. Chem.*, 2011, **21**, 17855.
36 G. Kalyuzhny, M. Buda, J. McNeill, P. Barbara and A. J. Bard, *J. Am. Chem. Soc.*, 2003, **125**, 6272.
37 H.-C. Su, H.-F. Chen, P.-H. Chen, S.-W. Lin, C.-T. Liao and K.-T. Wong, *J. Mater. Chem.*, 2012, **22**, 22998.
38 H.-B. Wu, H.-F. Chen, C.-T. Liao, H.-C. Su and K.-T. Wong, *Org. Electron.*, 2012, **13**, 483.
39 V. Jankus, C.-J. Chiang, F. Dias and A. P. Monkman, *Adv. Mater.*, 2013, **25**, 1455.
40 J. C. Deaton, S. C. Switalski, D. Y. Kondakov, R. H. Young, T. D. Pawlik, D. J. Giesen, S. B. Harkins, A. J. M. Miller, S. F. Mickenberg and J. C. Peters, *J. Am. Chem. Soc.*, 2010, **132**, 9499.

